J Mater Sci (2008) 43:3769–3774
DOI 10.1007/s10853-007-2157-x

INTERGRANULAR AND INTERPHASE BOUNDARIES IN MATERIALS

The approach to equilibrium during tempering of a bulk nanocrystalline steel: an atom probe investigation

F. G. Caballero · M. K. Miller · C. Garcia-Mateo

Received: 29 June 2007 / Accepted: 10 September 2007 / Published online: 6 March 2008

Abstract A local electrode atom probe has been used to analyze the solute partitioning during bainite transformation in a novel, nanocrystalline bainitic steel. Atom probe results show the absence of any partitioning of substitutional elements between the phases involved. The results are fully consistent with the diffusionless transformation of austenite to bainite. However, substitutional elements are expected to redistribute approaching an equilibrium phase boundary as the mixture of bainitic ferrite and retained austenite is tempered. The compositional analysis of the austenite/ferrite interface by atom probe tomography indicates that retained austenite decomposes during tempering before equilibrium is reached at the interface.

Introduction

Phase transformation theory has been used to create a steel in which the crystals of ferrite, embedded in a matrix of austenite are finer than that of carbon nanotubes. The microstructure is generated at temperatures, which are so low that iron diffusion does not occur during the austenite-to-ferrite transformation. The result is an extraordinary combination of strength and toughness (UTS of 2500 MPa and K_{IC} in excess of 30–40 MPam$^{1/2}$); the bainite has the highest hardness ever reported [1].

The bainite transformation progresses by the diffusionless growth of tiny platelets known as “sub-units”. One consequence of diffusionless growth in a bainitic transformation is that the plates can be supersaturated with carbon, in which case the carbon partitions into the residual austenite soon after the growth event. Diffusionless growth of this kind can only occur if the carbon concentration of the parent austenite is less than that given by the T'_{o} curve. The T_o curve is the locus of all points, on a temperature versus carbon concentration plot, where austenite and ferrite of the same chemical composition have the same free energy. The T'_{o} curve is defined similarly, taking into account the stored energy (400 J mol^{-1}) of the ferrite due to the displacive mechanism of transformation [2]. Consistent with thermodynamic theory, the carbon concentration of the austenite, as determined from X-ray analysis at the termination of the bainite reaction for different transformation temperatures, lies closer to the T'_{o} value boundary and far from the paraequilibrium phase boundary [3]. The reaction is said to be incomplete since transformation stops well before the phases achieve their equilibrium compositions.

In this work, a local electrode atom probe has been used to analyze the solute partitioning during bainite transformation in the novel, nanocrystalline bainitic steel described above. Moreover, the redistribution of substitutional elements approaching an equilibrium phase boundary has been examined as the mixture of bainitic ferrite and retained austenite is tempered.

F. G. Caballero (✉) · C. Garcia-Mateo
Centro Nacional de Investigaciones Metalúrgicas
(CENIM-CSIC), Avda Gregorio del Amo, 8, Madrid 28040,
Spain
e-mail: fgc@cenim.csic.es
URL: http://www.cenim.csic.es

M. K. Miller
Materials Science and Technology Division, Oak Ridge National
Laboratory (ORNL), P.O. Box 2008, Oak Ridge,
TN 37831-6136, USA
e-mail: millermk@ornl.gov
URL: http://www.ornl.gov/sci/share/

Table 1 Chemical composition

	C	Si	Mn	Mo	Cr	V
Wt.%	0.98	1.46	1.89	0.26	1.26	0.09
at.%	4.34	2.76	1.82	0.14	1.28	0.09

Experimental procedure

The chemical composition of the steel studied is given in Table 1. Homogenized specimens were austenitized for 15 min. at 1,000 °C, and then transformed to bainite at 200 °C for different times before quenching into water. The fully bainitic microstructure obtained at 200 °C for 144 h was tempered between 400 and 500 °C for 30 or 60 min.

The bainitic microstructure of the steel and its evolution during tempering were characterized by transmission electron microscopy (TEM) using thin foils electropolished at room temperature in a mixture of 5% perchloric acid, 15% glycerol and 80% methanol at 40 V until perforation occurred.

Retained austenite volume fraction in the microstructure was evaluated by X-ray experiments conducted on etched samples [4]. Moreover, austenite and ferrite carbon content were calculated from the measured lattice parameters [5–7].

Atom probe tomography specimens were electropolished using the standard double layer and micropolishing methods [8]. Atom probe analyses were performed in the ORNL local electrode atom probe operated at a specimen temperature of 60 K, a pulse repetition rate of 200 kHz, and a pulse fraction of 0.2.

Results and discussion

Low temperature bainite. Microstructural evolution during tempering

The evolution of phases present in the microstructure formed after isothermal transformation of austenite to bainitic ferrite at 200 °C at different time intervals are illustrated in graph and light optical micrographs of Fig. 1. After 24 h of holding time at 200 °C, bainite transformation has not started and a mixture of martensite and retained austenite is obtained by quenching (Fig. 1b). Martensitic plates are not parallel sided, instead they are lenticular as a result of constraints in the matrix which oppose the shape change resulting from the transformation. Another feature of higher carbon martensites illustrated in Fig. 1b is the burst phenomenon, in which one martensite plate nucleates a sequence of plates presumably as a result of stress concentrations set up when the first plate reaches an obstruction such as a grain boundary or another martensite plate.

A longer isothermal transformation time (48 h) at 200 °C was required to obtain a significant amount of bainite, as shown in Fig. 1c. The plates of bainite grow in clusters called sheaves. Within each sheaf of bainite, the

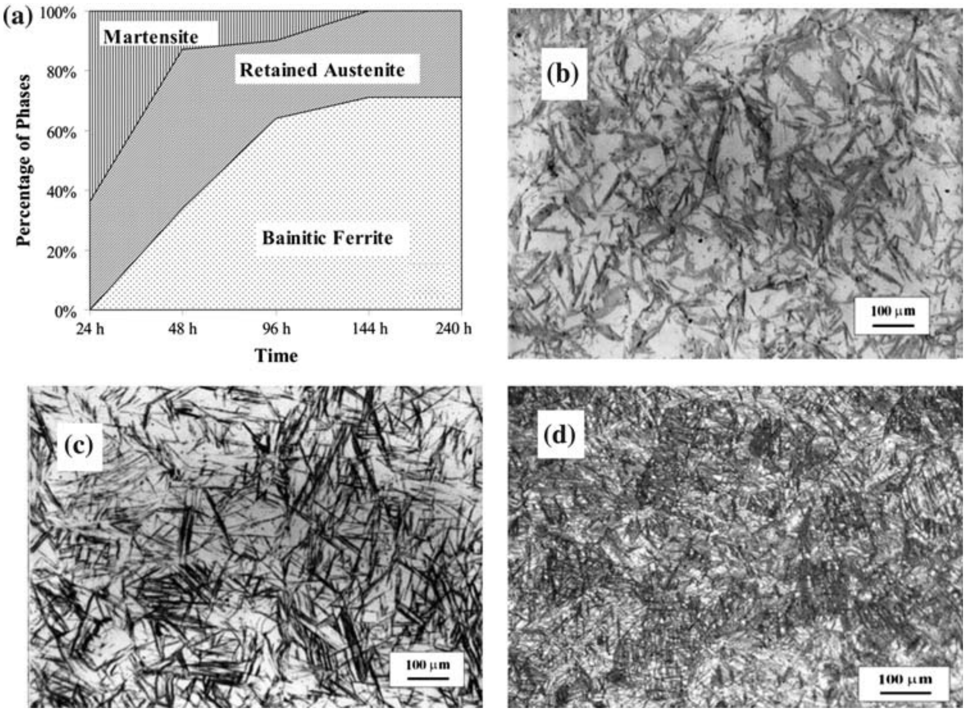

Fig. 1 (**a**) Phase fraction evolution during isothermal transformation at 200 °C for several times, and (**b**), (**c**) and (**d**) Light optical micrographs of the microstructure formed at 200 °C for 24, 48 and 144 h, respectively

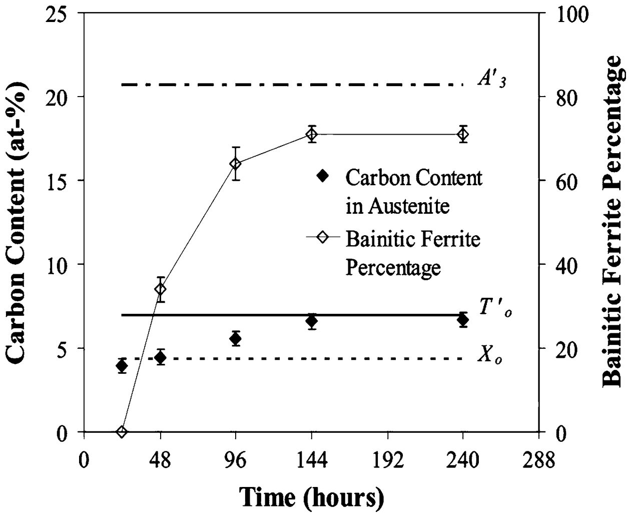

Fig. 2 Evolution of the carbon content in retained austenite as bainite transformation progresses at 200 °C. X_o represents the overall carbon content of the steel. T'_o and the paraequilibrium A'_3 curves were calculated for the studied steel [8]

plates are parallel and of identical crystallographic orientation, each with a well-defined crystallographic habit. The individual plates in a sheaf are often called sub-units of bainite. They are usually separated by low-misorientation boundaries. Bainite reaction stopped after holding for 144 h, leaving untransformed austenite (Fig. 1d).

X-ray analysis results on the evolution of carbon in austenite during transformation at 200 °C are shown in Fig. 2. The measured concentrations in austenite lie closer to the T'_o value boundary [9] and far from the paraequilibrium phase boundary. This trend is consistent with a mechanism in which the bainite grows without any diffusion, but with excess carbon partitioning into the austenite soon after transformation. The reaction is said to be incomplete since transformation stops before the phases achieve their equilibrium compositions.

The TEM micrograph in Fig. 3a shows the fully carbide-free bainitic microstructure formed at 200 °C. It is well known that the presence of silicon retards the precipitation of cementite from austenite during bainite formation, because of its low-solid solubility in the cementite crystal structure [10–14]. Thus, the carbon that is rejected from the bainitic ferrite enriches the residual austenite, thereby stabilizing it down to ambient temperature. The resulting microstructure consists of fine plates of bainitic ferrite separated by carbon-enriched regions of austenite.

Quite remarkably, bainitic plates formed at low temperature (200 °C) are long and thin with a width that is less than 50 nm. Each plate is separated by very thin films of retained austenite giving this novel nanostructured bainitic microstructure (Fig. 3a). The plate thickness mainly depends on the strength of the austenite and the free energy change accompanying transformation [15]. The observed refinement is a consequence mainly of the high carbon content and the low transformation temperature on enhancing the strength of the austenite.

Tempering for 1 h at 400 °C did not introduce appreciable changes in the initial microstructure. Extremely fine plates of ferrite and thin films of retained austenite were still observed (see TEM micrograph in Fig. 3b). The austenite volume fraction also did not change. X-ray analysis estimate yielded a volume fraction of 0.29 ± 0.01.

At 450 °C for 30 min (see TEM micrograph in Fig. 3c), most of the retained austenite has decomposed into cementite and ferrite. X-ray analysis showed that the volume fraction of austenite decreases from 0.29 to 0.02. Complete decomposition of retained austenite occurs as temperature increases. Therefore, austenite is no longer present in the tempered microstructure; the microstructure tempered at 500 °C is not analyzed in this study.

Solute distribution during bainite formation

A 5 at.% carbon isoconcentration plot of an austenite–ferrite interface for the transformation temperature of 200 °C and two examples of carbon atom maps of the interface after tempering are shown in Fig. 4. The corresponding elemental concentration profiles across the interface are represented in Fig. 5. The 5 at.% carbon isoconcentration surface shown in Fig. 4a and the elemental concentration profiles across the interface in the initial microstructure (Fig. 5) indicate that the distribution of carbon atoms in the analysis volume is not uniform and carbon-rich and carbon-depleted regions are clearly distinguishable in the material that is fully transformed to

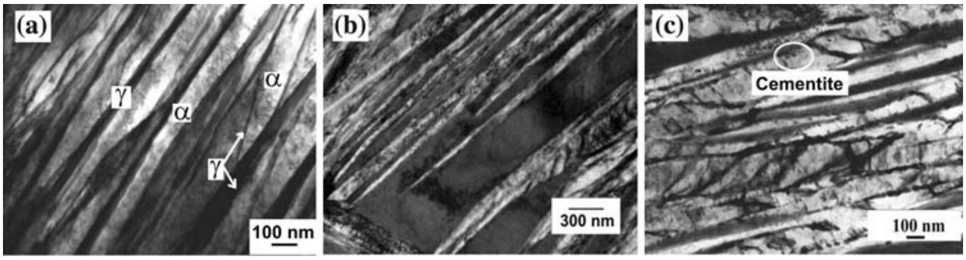

Fig. 3 Transmission electron micrographs of microstructure obtained (**a**) at 200 °C at the termination of the bainite reaction, and after tempering at (**b**) 400 °C for 1 h and (**c**) 450 °C for 30 min

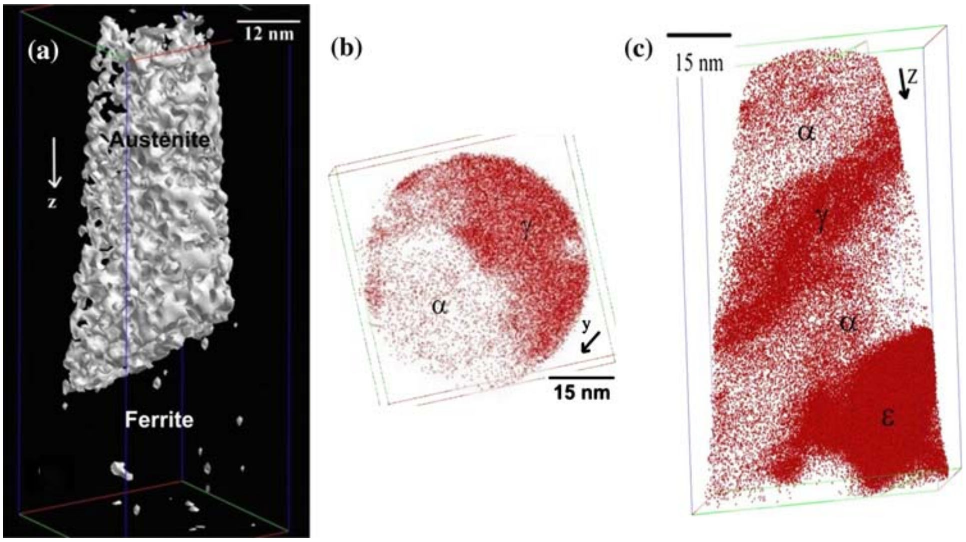

Fig. 4 (**a**) 5 at.%C—isoconcentration surface of austenite/bainitic ferrite interface during bainite formation at 200 °C. Carbon atom maps of austenite/bainitic ferrite interface after tempering at (**b**) 400 °C for 1 h and (**c**) 450 °C for 30 min. α is ferrite, γ is austenite, and ε is ε-carbide

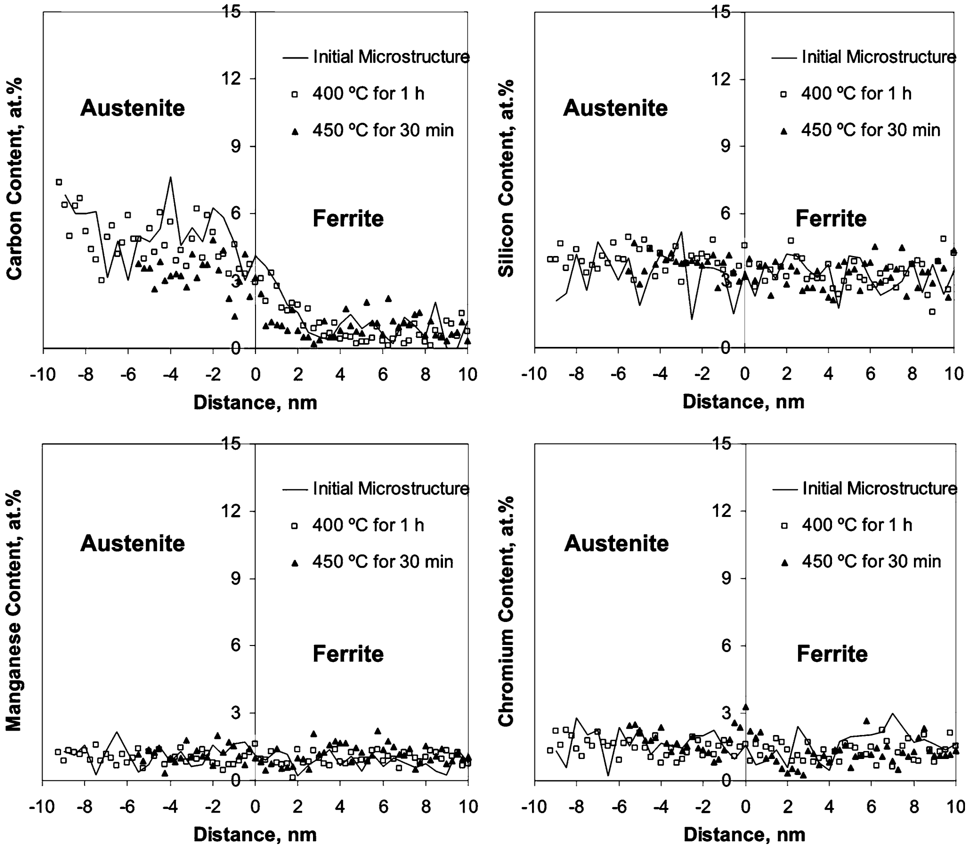

Fig. 5 Evolution of elemental concentration profiles across austenite/bainitic ferrite interface after tempering

bainite at 200 °C. The carbon-enriched region represents austenite as its carbon content is higher than the average value of 4.3 at.% and the low carbon (<1 at.%) region indicates the ferrite phase.

It is important to note these atom probe data reveal the presence of carbon-enriched austenite (5.39 ± 0.18 at.%) and carbon-depleted ferrite (0.62 ± 0.10 at.%), which is consistent with earlier work [16]. Quantitative data for the initial microstructure (Fig. 5) also confirms the absence of any partitioning of substitutional elements such as silicon, manganese and chromium between the phases involved. The results are fully consistent with the diffusionless transformation of austenite to bainite [17].

In most cases, the atom probe results on carbon content of both bainitic ferrite and austenite are lower than those measured by X-ray. This is because the atom probe estimate is a simple counting of atoms within the selected volume of matrix of ferrite or austenite that does not contain any carbon enriched regions such as dislocations and boundaries and not an average of a larger volume that may be enriched in carbon as in the X-ray estimate.

It is also clear from the atom probe data for the initial microstructure that there is no significant segregation of either substitutional elements or carbon to the austenite–ferrite interface. The absence of any significant solute build-up at the interface indicates that the interface may not provide a very large sink for atoms since the interface involved must be semi-coherent, with a high degree of coherency, consistent with the shape change effect [16].

The crystallographic theory of martensite is based on the postulation that the habit plane is an invariant plane relative to the macroscopic shape deformation. The parent–product mismatch at the habit plane is considered to be periodically corrected by discontinuities so that the misfit in the interface plane does not accumulate over large distance [18]. These structural discontinuities are needed only to correct the mismatch at the semi-coherent planar boundary. However, for lenticular plates exhibiting a curved boundary, this interface is glissile since the additional misfit regions arising from the boundary curvature constitute the transformation dislocations of the martensite pole mechanism [19]. Since the sub-units of bainitic ferrite have a lenticular plate morphology [20], their interfaces with austenite must also be glissile, in accord with a displacive transformation mechanism. By examining the interface mobility, Bhadeshia [21] provided strong evidence to suggest that the interface which accomplished bainitic transformation in steels is glissile. He demonstrated that the mobility of an interface whose motion does not lead to the formation of invariant-plane strain surface relief effects is extremely slow at temperatures where bainite forms.

Redistribution of alloying elements during tempering

As mentioned above, there is no partitioning of substitutional solutes during the bainite reaction. Given the opportunity, the solutes should tend to redistribute in a manner that leads to a reduction in the overall free energy. It is found that when a mixture of bainitic ferrite and retained austenite is tempered at low temperatures, the solutes partition before the austenite begins to decompose [22].

The carbon atom map in Fig. 4b shows an austenite–ferrite interface after tempering at 400 °C for 1 h. Corresponding elemental concentration profiles (Fig. 5) across the interface suggest that no partitioning of substitutional elements occur after this tempering condition. The carbon content in the austenite (5.16 ± 0.88 at.%) and in the ferrite (0.57 ± 0.35 at.%) are similar to that measured in the initial microstructure (Fig. 5). Results confirm that tempering for 1 h at 400 °C did not introduce any change in the original microstructure, even at the atomic level.

Table 2 Concentration of austenite and ferrite in equilibrium from MTDATA, at.%

Temperature (°C)	Phase	C	Cr	Mn	Si	Mo	V	Fe
400	Austenite	16.71	0.24	4.36	0.35	–	–	78.34
	Ferrite	0.05	–	0.08	3.19	–	–	96.68
450	Austenite	14.98	0.43	8.58	0.52	–	–	75.48
	Ferrite	0.05	–	0.31	3.31	–	–	96.32

The carbon atom map of an austenite–ferrite interface for the material tempered at 450 °C for 30 min is shown in Fig. 4c, where ε-carbide was also detected within the ferrite. Corresponding elemental concentration profiles are represented in Fig. 5. As X-ray analysis suggested, at this stage, appreciable amounts of retained austenite decompose (i.e., cementite precipitation), which would explain the decreases in the carbon content in the austenite (3.75 ± 0.95 at.%) detected by atom probe tomography (Fig. 5). TEM observations and atom probe tomography data showed that cementite precipitation occurred after tempering at 400 °C for 1 h.

Apart from carbon, chromium is the only solute that partitions across the austenite–bainitic ferrite interface. It is clear from the chromium concentration profile that the chromium spikes at the austenite/bainitic ferrite interface. An elemental spike usually indicates that negligible partitioning local equilibrium (NPLE) is reached at the interface. There is no clear indication of silicon or manganese partitioning across the austenite–bainitic ferrite interface.

The equilibria between austenite and ferrite (Table 2) were determined using the MTDATA thermodynamic computer program [23]. Comparison of the experimentally observed alloying element redistributions determined from atom probe tomography and the thermodynamic calculations indicates that retained austenite decomposes before local equilibrium is reached at the interface.

Conclusions

Atom probe tomography has been used to analyze the solute partitioning during bainite transformation in a novel, nanocrystalline bainitic steel. Atom probe results confirm the absence of any partitioning of substitutional elements between the phases. However, substitutional elements are expected to redistribute approaching an equilibrium phase boundary as the mixture of bainitic ferrite and retained austenite is tempered. The compositional analysis of the austenite/ferrite interface at an atomic scale indicates that retained austenite decomposes during tempering before equilibrium is reached at the interface.

Acknowledgements The authors acknowledge financial support from European Coal and Steel Community (ECSC 7210-PR-345) and Spanish Ministerio de Ciencia y Tecnología (Project-2006 6 0I 029). CGM would also like to thank Spanish Ministerio de Ciencia y Tecnología for the financial support in the form of a Ramón y Cajal contract (Programa RyC 2004). Research at the Oak Ridge National Laboratory SHaRE User Facility was sponsored by the Office of Basic Energy Sciences, Division of Scientific User Facilities, U.S. Department of Energy, under contract DE-AC05-00OR22725 with UT-Battelle, LLC.

References

1. Caballero FG, Bhadeshia HKDH, Mawella JA, Jones DG, Brown P (2002) Mater Sci Tech 18:279
2. Bhadeshia HKDH (1981) Acta Metall 29:1117
3. Bhadeshia HKDH, Edmonds DV (1979) Metall Trans 10A:895
4. Caballero FG, Miller MK, Babu SS, Garcia-Mateo C (2007) Acta Mater 55:381
5. Dyson DJ, Holmes B (1970) J Iron Steel Inst 469
6. Bhadeshia HKDH, David SA, Vitek JM, Reed RW (1991) Mater Sci Tech 7:686
7. Cullity BD, Stock SR (2001) Elements of X-ray diffraction, 3rd edn. Prentice Hall, Upper Saddle River, p 411
8. Miller MK (2000) Atom probe tomography. Kluwer Academic/Plenum Press, New York, p 28
9. http://www.msm.cam.ac.uk/map/steel/programs/mucg46-b.html
10. Matas SJ, Hehemann RF, (1961) Trans Met Soc AIME 221:179
11. Entin R (1962) In: Zackay VF, Aaronson HI (eds) Decomposition of austenite by diffusional processes. Interscience, New York, p 295
12. Hehemann RF (1970) Phase transformations. American Society for Metals, Metals Park, Ohio, p 397
13. Lyman T, Troiano AR (1945) Trans Met Soc AIME 162:196
14. Lehouillier R, Begin G, Dube A (1971) Metall Trans 2A:2645
15. Singh SB, Bhadeshia HKDH (1998) Mat Sci Eng A 245:72
16. Bhadeshia HKDH, Waugh AR (1982) Acta Metall 30:775
17. Bhadeshia HKDH, Edmonds DV (1980) Acta Metall 28:1265
18. Christian JW (1979) Phase transformations, vol 1, no 11, series 3. Institute of Metallurgists, London, p 1
19. Christian JW (1965) The theory of transformations in metals and alloys. Pergamon Press, Oxford
20. Bhadeshia HKDH, Christian JW (1990) Metall Trans 21A:767
21. Bhadeshia HKDH (1982) J Phys Colloq C4 43:C4–443
22. Stark I, Smith GDW, Bhadeshia HKDH (1990) Metall Mater Trans 21A:847
23. MTDATA (2003) Phase diagram calculation software. National, Physical Laboratory, Teddington